Atmos. Meas. Tech., 18, 6645–6657, 2025 https://doi.org/10.5194/amt-18-6645-2025 © Author(s) 2025. This work is distributed under the Creative Commons Attribution 4.0 License.





# Laboratory characterization of furan, 2(3H)-furanone, 2-furaldehyde, 2,5-dimethylfuran, and maleic anhydride measured by PTR-ToF-MS

Wade Permar, Mercedes Tucker, and Lu Hu

Department of Chemistry and Biochemistry, University of Montana, Missoula, MT, USA

**Correspondence:** Wade Permar (wade.permar@mso.umt.edu)

Received: 20 June 2025 – Discussion started: 27 June 2025

Revised: 16 September 2025 – Accepted: 29 September 2025 – Published: 18 November 2025

Abstract. Furanoids are significant contributors to volatile organic compound hydroxyl radical reactivity in biomass burning emissions, yet their accurate measurement using proton-transfer-reaction time-of-flight mass spectrometry (PTR-ToF-MS) remains challenging due to potential interferences and measurement uncertainties. In this study, we conduct detailed laboratory characterizations of furan  $(C_4H_4O, protonated m/z 69.033), 2(3H)$ -furanone  $(C_4H_4O_2, protonated m/z 69.033), 2(3H)$ m/z 85.028), 2-furaldehyde (C<sub>5</sub>H<sub>4</sub>O<sub>2</sub>, m/z 97.028), 2,5dimethylfuran ( $C_6H_8O$ , m/z 97.065), and maleic anhydride  $(C_4H_2O_3, m/z 99.008)$ . Sensitivities for these compounds were found to have minimal dependence (less than 15 %) on both sample humidity and drift tube electric field strength (E/N). At high E/N (150 Td), fragmentation was observed for 2-furaldehyde ( $\sim$  8 %) at m/z 69.033, potentially interfering furan measurements, while hydrolysis products corresponding to m/z + 18 ions were detected for 2(3H)-furanone, 2furaldehyde, and maleic anhydride. The hydrolysis of maleic anhydride to maleic acid is most prominent, with the hydrate accounting for 7 %-31 % of the parent ion signal across E/N conditions.

Gas standard recertification confirmed the long-term stability of furanoids, and 21 other VOCs, in compressed gas mixtures, with changes in mixing ratios of less than  $5\,\%$  over seven years, although PTR-ToF-MS instrument sensitivities decreased by  $\sim 30\,\%$  during this time, likely due to aging of the microchannel plate (MCP). While the stability of gas standards and the minimal humidity and fragmentation effects support the accurate measurement of furanoids by PTR-ToF-MS, discrepancies with co-deployed gas chromatography-mass spectrometry highlight the need to

further investigate potential isomeric and fragment interferences, particularly in aged BB smoke.

#### 1 Introduction

Furanoids, a class of volatile organic compounds (VOCs) consisting of a five-member ring with four carbons and one oxygen, are primarily emitted to the atmosphere from biomass burning (BB) (Akagi et al., 2011; Gkatzelis et al., 2024; Koss et al., 2018; Permar et al., 2021). Additional minor emission sources include volatile chemical products (McDonald et al., 2018), flavorings and food (Crews and Castle, 2007), vehicles (Wang et al., 2022), and biofuels (Román-Leshkov et al., 2007; Tuan Hoang and Viet Pham, 2021). Due to their high reactivity with OH and NO<sub>3</sub> radicals, furanoids can substantially contribute to atmospheric oxidation capacity and influence ozone (O<sub>3</sub>) and secondary organic aerosol (SOA) formation (Coggon et al., 2019; Joo et al., 2019; Romanias et al., 2024).

In wildfire smoke, furanoids constitute a significant OH sink, accounting for  $\sim\!20\,\%$  of a smoke plume's initial OH reactivity and up to  $10\,\%$  of near field O<sub>3</sub> production (Coggon et al., 2019; Gilman et al., 2015; Koss et al., 2018; Permar et al., 2023). Prominent contributors include C<sub>2</sub> substituted furans, 2-furaldehyde, furan, methyl furfurals, and furanone (Koss et al., 2018; Permar et al., 2023). Despite the atmospheric lifetime of many of these species being only a few hours, furanoids remain an important OH sink ( $\sim\!10\,\%$  of plume OH reactivity) in smoke aged beyond three days due to the production of more oxygenated species such as

2-furoic acid/5-hydroxy-2-furfural ( $C_5H_4O_3$ ), succinic anhydride ( $C_4H_4O_3$ ), and maleic anhydride ( $C_4H_2O_3$ ) (Permar et al., 2023).

Furanoids are increasingly being used as BB tracers, particularly in mixed urban/smoke environments where acetonitrile can be less reliable (Bruns et al., 2017; Huangfu et al., 2021). Maleic anhydride is of particular interest due to its atmospheric lifetime of more than 5 d and it being formed primarily from furan oxidation (Coggon et al., 2019; Romanias et al., 2024). Shorter lived compounds such as furan and methyl furan are also useful indicators of smoke age and transport due to their lack of secondary production (Gkatzelis et al., 2024; Liang et al., 2022; O'Dell et al., 2020; Rickly et al., 2023; Robinson et al., 2021).

However, PTR-ToF-MS measurements of furanoids in fresh wildfire smoke have been observed to differ substantially from gas chromatography-based techniques, with PTR-ToF-MS reporting  $\sim 1.5$ –2 times more furan and up to 15 times more methyl furans than the gas chromatography-based Trace Organic Gas Analyzer (TOGA) (Gkatzelis et al., 2024; Permar et al., 2021). These discrepancies exist even after being corrected for known interferences based on laboratory characterization (Koss et al., 2018), suggesting that unresolved fragmentation or isomeric overlaps may still bias measurements.

While recent studies have expanded the list of detectable furanoids, sensitivities for most species are based on kinetically determined calibration factors with uncertainties up to 50 % (de Gouw and Warneke, 2007; Sekimoto et al., 2017). Furthermore, it is assumed that these species have little to no fragmentation in PTR-MS, which has not been rigorously tested for most furanoids. A recent review by Romanias et al. (2024) has extensively described the current state of the science for many atmospheric reactions of furanoids, but notes that PTR-ToF-MS "faces limitations in accurately quantifying furanoids, particularly in the presence of interfering compounds and under varying environmental conditions. Resolving these challenges requires comprehensive laboratory investigations to elucidate the fundamental properties of furanoids and develop robust analytical methods for their detection and quantification."

Here, we present detailed laboratory characterizations of five atmospherically relevant furanoids: furan, 2(3H)-furanone, 2-furaldehyde, 2,5-dimethylfuran, and maleic anhydride. Our investigation encompasses the fragmentation, humidity dependence, and electric field-dependent sensitivities of these key VOCs in PTR-ToF-MS measurements. Additionally, we assess the long-term stability (7 years) of select furanoid gas standards. These results close important measurement gaps by showing that PTR-ToF-MS sensitivities are largely unaffected by humidity or electric field conditions, and that gas standards can remain stable over multiple years. By ruling out these potential sources of bias, our findings indicate that remaining discrepancies most likely stem from unresolved issues with speciation and interferences in com-

plex airmass, highlighting the need for further identification work.

#### 2 Methods

#### 2.1 Insturment description

Laboratory calibrations of furan ( $C_4H_4O$ , protonated m/z 69.033), 2(3H)-furanone ( $C_4H_4O_2$ , m/z 85.028), 2-furaldehyde ( $C_5H_4O_2$ , m/z 97.028), 2,5-dimethylfuran ( $C_6H_8O$ , m/z 97.065), and maleic anhydride ( $C_4H_2O_3$ , m/z 99.008) were carried out using a proton-transferreaction time-of-flight mass spectrometer previously described in detail by Permar et al. (2021).

Briefly, in PTR-ToF-MS, VOCs with proton affinities greater than water (691 kJ mol<sup>-1</sup>) are ionized via proton transfer reaction with  $\rm H_3O^+$  reagent ions in the instrument's drift tube (Reaction R1). Most VOCs, including furanoids, have proton affinities greater than water, while the major constituents of air such as N<sub>2</sub>, O<sub>2</sub>, and CO<sub>2</sub> do not. Consequently, PTR-ToF-MS can measure hundreds to thousands of different VOCs in real time with no sample pretreatment at up to 10 Hz. The proton transfer reaction is also a soft ionization technique which typically results in little fragmentation of the analyte ions, allowing for them to be detected at their protonated mass (m/z+1). However, fragmentation can still occur, particularly with compounds that readily dehydrate or form stable intermediate cations (Coggon et al., 2024).

$$H_3O^+ + VOC \rightarrow VOC \cdot H^+ + H_2O$$
 (R1)

The efficiency of the proton transfer reaction is controlled by the drift tube energy, described as the E/N in Td. E/N is itself a product of drift tube temperature, pressure, and voltage, with higher E/N corresponding to increased collisional energy. Generally, higher E/N results in greater instrument sensitivity as more analyte is protonated and clustering with excess H<sub>2</sub>O is decreased (de Gouw and Warneke, 2007; Yuan et al., 2017). However, higher collisional energy can also cause more compounds to fragment, increasing the difficulty to identify and quantify the full mass spectrum. Optimal drift tube conditions then are a balance between getting sufficient sensitivities for analytes of interests while minimizing their fragmentation. As molecular structure, polarity, dipole, and functional groups all play a role in a compound's sensitivity and propensity to fragment, optimal E/N conditions can vary based on the analyte of interest.

In addition to sensitivity being dependent on instrument drift tube energy, the presence of excess water vapor in a sample can also impact the efficiency of the proton transfer reaction. Typically, the impact of humidity on instrument sensitivities is greatest for VOCs with proton affinities nearer to water, as the reverse reaction becomes more competitive (Reaction R1), leading to a decrease in measurement sensitivity. In PTR-MS, the ratio of water clusters to the pri-

mary ion ([ $H_2O(H_3O^{18})$ +]/[ $H_3O^{18}$ +] or m39 / m21) is used as a proxy to estimate the humidity in the drift tube due to their linear relationship with relative humidity (de Gouw and Warneke, 2007; Stönner et al., 2016), and typically maintained at less than 5 %. Previous studies have shown the m39 / m21 ratio can be used to derive humidity dependent sensitivities for VOCs with lower proton affinities (Baasandorj et al., 2015; Warneke et al., 2011a).

#### 2.2 Standard preparation and calibration system

Calibrations were conducted using a syringe pump with liquid standard prepared from furanoid standards diluted to 100-300 ppm in analytical grade ethyl acetate. Ethyl acetate was chosen for use as a solvent due to maleic anhydride and 2(3H)-furanone being reactive with water making it so neither water nor alcohols (which typically absorb water) could be used. Similarly, dimethylfuran is not miscible in water, while typical non-polar solvents such as cyclohexane and n-hexanes were found to have strong interference at m/z 69 due to either uncharacterized fragments and/or contamination in the solvent, even for commercially available analytical grade products.

Ethyl acetate has a proton affinity of 835.7 kJ mol<sup>-1</sup> and is therefore detectable by PTR-MS at m/z 89.060. When used as a solvent, ethyl acetate has high enough concentrations to saturate the instrument signal at m/z 89. The mass spectra of the pure ethyl acetate solvent also have notable peaks at m/z 43, 61, 79, and 107, likely due to fragmentation and contamination. Peaks from the <sup>13</sup>C and <sup>18</sup>O isotopes are also present. However, we found no overlap with the ethyl acetate solvent peaks and any of the furanoid compounds, nor any depletion of the primary ion. To account for shifts in the base line caused by the high ethyl acetate signal and presence of contaminate peaks, the instrument background was corrected across the range of solvent flows for each calibration. Additionally, raw counts are normalized to H<sub>3</sub>O<sup>+</sup> to account for variation in the instrument's primary ion signal and expressed here as normalized counts per second per ppb (NCPS  $ppb^{-1}$ ) (de Gouw and Warneke, 2007).

Standard additions were conducted using a custom-built syringe pump based calibration system (Fig. 1). The system works by injecting  $50\text{--}150\,\text{nl}\,\text{min}^{-1}$  of liquid standard into  $500\,\text{sccm}$  of catalyst generated zero via a syringe pump (Harvard Apparatus PHD ULTRA) equipped with a  $10\,\mu\text{L}$  Hamilton gastight syringe. The standard is immediately evaporated into the zero air, and then further diluted and humidified in a heated chamber ( $100\,^{\circ}\text{C}$ ) by mixing with  $1000\,\text{sccm}$  of zero air and  $0\text{--}50\,\mu\text{L}\,\text{min}^{-1}$  of water, vaporized via a nebulizer. The PTR-ToF-MS inlet subsamples the humidified standard with excess flow going to the exhaust. Using this method, we can make sub-ppb standards, with most calibrations in this work carried out from  $0.8\text{--}3\,\text{ppb}$ .

The efficacy of the syringe pump system was validated by comparison to sensitivities determined from both compress gas standards and a commercially available Liquid Calibration Unit (LCU, Ionicon Analytik). Additionally, all syringe pump calibrations were carried out using acetonitrile as an internal standard at approximately the same concentrations as the furanoid of interest. For each furanoid calibration, the sensitivity for acetonitrile was also calculated and found to consistently be in good agreement with its sensitivity from compressed gas standard calibrations. Data when acetonitrile sensitivities varied by greater than 10 % were removed from further analysis, providing a per-sample check on the syringe pump's performance.

#### 2.3 Compressed gas standards

In addition to the calibrations done in this work using liquid standards, we also examined the stability of two seven-year-old compressed gas cylinders (Apel-Riemer Environmental, Inc.) that contain  $\sim 1$  ppm each of furan, 2-furaldehyde, 2-methylfuran, and 5-methylfurfural, along with 21 other VOCs (Table A1). Both cylinders were originally prepared in 2017 and recertified by the manufacturer in 2024. Standards are gravimetrically prepared in cleaned, treated, high-pressure aluminum cylinders from traceable liquid standards. Accuracy is better than  $\pm 5\,\%$ , with GC-MS analysis confirming the accuracy of the gravimetric preparation and recertification concentrations. Cylinders are certified for 36 months, though many compounds are stable for several years.

#### 2.4 Fragmentation and E/N dependence

For each furanoid, the extent of fragmentation was first determined by identifying the major ion peaks at  $\sim 10\,\mathrm{ppb}$  of standard generated by the syringe system described above. Fragmentation was then probed at E/N of 110 and 150 Td, set by changing the drift tube voltage from 660 to 900 V while maintaining a constant temperature and pressure (60 °C, 3.0 mbar). We limit our analysis to E/N 110–150 Td as we are no longer able to control the m39 / m21 ratio within the desired 0 %–5 % outside this range. Instrument background was then determined using a constant injection of ethyl acetate followed by a constant injection of liquid standard. Humidity was controlled to maintain m39 / m21 at 2.5 %–3.0 %. Fragments were then identified as masses with average normalized counts greater than three times the standard deviation of the background signal (3 $\sigma$ ).

For all humidity dependent experiments, drift tube conditions were maintained at 810 V, 60 °C, and 3.00 mbar (E/N = 134 Td), which is the standard conditions used for our instrument during ambient sampling (Permar et al., 2021; Selimovic et al., 2022; Cope et al., 2024). Four-point calibrations were then conducted while adjusting the humidity of the carrier gas such that the m39 / m21 ratio changed from 0.2 % to 8 %, at  $\sim$  0.5 % increments. Similarly, to determine how each species sensitivity depends on electric field strength, four-point calibrations were carried out at E/N

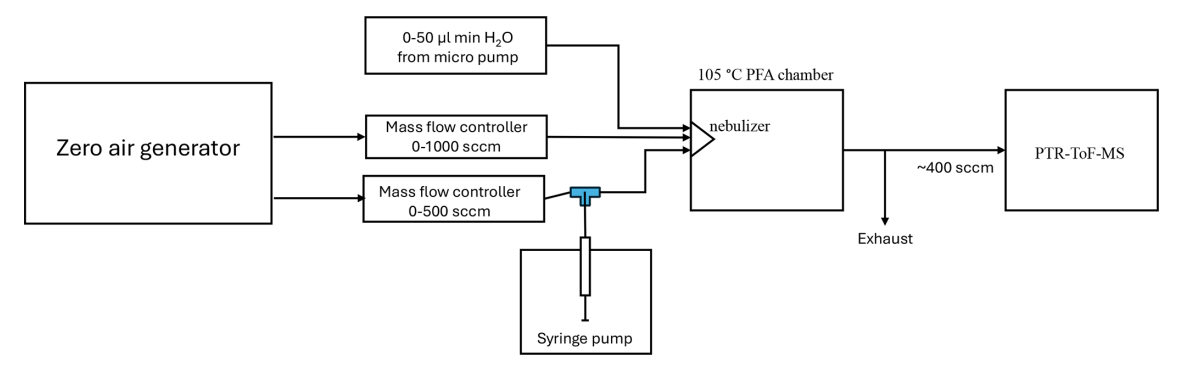


Figure 1. Schematic of the syringe pump based calibration system used in this work.

 $110\text{--}150\,\mathrm{Td}$  stepped at  $\sim\!5\,\mathrm{Td}$ . This was done by varying the electric field strength of the drift tube from 660–900 V while maintaining constant pressure and temperature. As the m39 / m21 ratio is also dependent on the electric field strength, the humidity of the carrier gas was increased in proportion to the E/N to maintain m39 / m21 at 2.5 %–3.0 % across all calibrations.

#### 3 Results

#### 3.1 Fragmentation

Furan and dimethylfuran were both found to have minimal drift tube chemistry or fragmentation and are consequently detected at their parent ion masses across all E/N in this work (Table 1, Fig. 2). 2-furaldehyde, 2(3H)-furanone, and maleic anhydride were found to have notable fragmentation to ions other than the parent mass, especially at high E/N (Fig. 2). For 2-furaldehyde, at 110 Td only the parent ion is detected at m/z 97.028, while at 150 Td m/z 69.033 accounts for 17% of the signal. This likely corresponds to a C<sub>4</sub>H<sub>4</sub>OH<sup>+</sup> ion forming from dehydration and subsequent fragmentation at the aldehyde group, similar to what has been observed in other long chain aldehydes (Coggon et al., 2024; Pagonis et al., 2019). This is of note as m/z 69.033 is commonly attributed to only furan (Koss et al., 2018; Pagonis et al., 2019; Yuan et al., 2017), meaning the fragmentation of 2-furaldehyde could bias PTR-ToF-MS furan measurements high in BB smoke where 2-furaldehyde and furan are emitted at similar rates (Koss et al., 2018; Permar et al., 2021). However, at our standard operating conditions (E/N 134, m39 / m21 < 5%) this contribution is only  $\sim$  8% of the parent ion signal. As PTR-ToF-MS and GC based measurements of furan differ by nearly 60 % in recent aircraft field campaigns (Gkatzelis et al., 2024; Permar et al., 2021), the fragmentation of 2-furaldehyde alone does not fully explain the discrepancy.

Maleic anhydride does not show evidence of fragmentation but is instead hydrolyzed via reaction with  $H_2O$  and detected at m/z 117.018. This reaction likely corresponds to

maleic anhydride being converted to maleic acid. At 110 Td, the hydrolysis reaction is minor with maleic acid only being 7% of the parent ion signal. This increases to 31% at 150 Td as the increased ionization energy makes the reaction more favorable. This product does not interfere with any atmospherically relevant VOCs described at m/z 117.018.

In aged BB smoke, succinic anhydride ( $C_4H_2O_3$ ) is also an important OH radical sink formed during the oxidation of furanoids (Coggon et al., 2019; Permar et al., 2023). Succinic anhydride has a similar chemical structure to maleic anhydride, with both rapidly converting to dicarboxylic acids in the presence of  $H_2O$ . We do not calibrate succinic anhydride in this work but hypothesize that due to also being an anhydride it will have similar drift tube chemistry as maleic anhydride. Succinic anhydride is detected at m/z 101.023 while its hydrolysis product, succinic acid ( $C_4H_6O_4$ ), would be detected at m/z 119.034. No notable VOCs measured by PTR-ToF-MS have been described at this mass.

2(3H)-furanone and 2-furaldehyde also exhibit m/z + 18peaks at high E/N (m/z 103.039 and 115.039 respectively), though only accounting for 7% and 5% of their parent ion masses respectively. The m/z + 18 product from 2(3H)furanone may interfere with the measurement of acetic anhydride (m/z 103.039), while that from 2-furaldehyde corresponds to 5-hydroxymethyl-2(3H)-furanone (m/z 115.039) (Koss et al., 2018). The exact mechanism leading to these ions is currently unknown. Given that higher E/N generally results in less clustering (de Gouw and Warneke, 2007) and that the m/z + 18 ion is not present in furan or dimethylfuran samples, it is unlikely to be due to simple clustering with H<sub>3</sub>O<sup>+</sup> alone. Instead, we hypothesize that the carbonyl groups follow the mechanism for nucleophilic addition of water (hydration) under acidic conditions to form a gem-diol. It is also possible that 2(3H)-furanone follows similar hydrolysis chemistry as maleic anhydride, with the furan ring opening to form alcohol and carboxylic acid functional groups.

#### 3.2 Humidity and E/N dependent sensitivity

To investigate furanoid sensitivity dependence on humidity, calibrations were carried out with the m39/m21 hu-

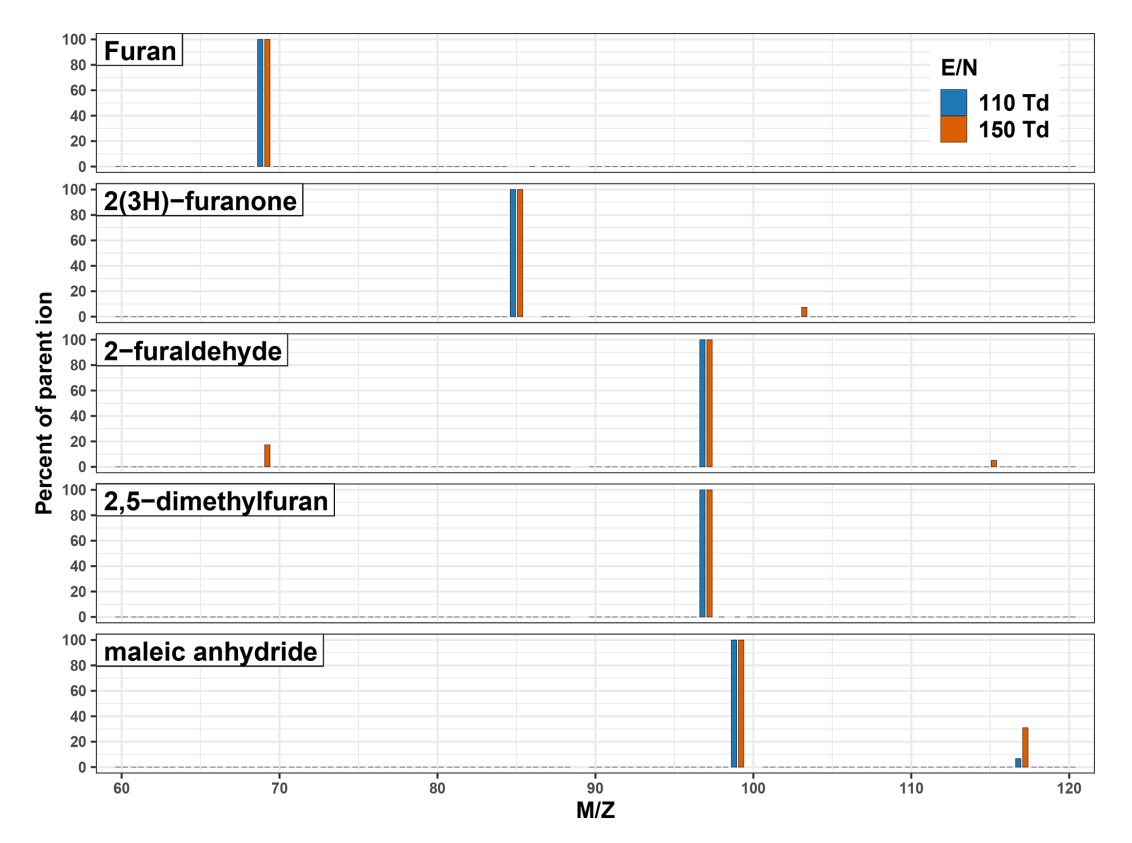


**Figure 2.** Major ion masses detected when measuring furan, 2(3H)-furanone, 2-furaldehyde, 2,5-dimethylfuran, and maleic anhydride at E/N of 110 Td (blue bars) and 150 Td (orange bars). Each bar corresponds to measured ions with average normalized counts greater than  $3\sigma$  the background signal.

**Table 1.** Summary of the humidity and electric field dependent sensitivity changes for the furanoids analyzed in this work, along with their major fragment ions as a proportion of their primary ion signal.

| Sensitivity changes as a product of: |                                 |                       |                          |                     |                                    |                |                       |  |
|--------------------------------------|---------------------------------|-----------------------|--------------------------|---------------------|------------------------------------|----------------|-----------------------|--|
| Species                              | Formula                         | Parent ion mass $m/z$ | m39 / m21<br>(0.2 %–8 %) | E/N<br>(110–150 Td) | Fragments<br>and other<br>products | Fragment $m/z$ | Percent of parent ion |  |
| furan                                | C <sub>4</sub> H <sub>4</sub> O | 69.033                | -14%                     | -2%                 | _                                  | _              | _                     |  |
| 2-(3H)furanone                       | $C_4H_4O_2$                     | 85.028                | -1%                      | -7%                 | $C_4H_6O_3H^+$                     | 103.039        | 0 %-7 %               |  |
| 2-furaldehyde                        | $C_5H_4O_2$                     | 97.028                | 12 %                     | -6%                 | $C_4H_4OH^+$                       | 69.033         | 0 %-17 %              |  |
| •                                    |                                 |                       |                          |                     | $C_5H_6O_3H^+$                     | 115.039        | 0 %-5 %               |  |
| 2,5-dimethylfuran                    | $C_6H_8O$                       | 97.065                | 6 %                      | -7%                 | _                                  | _              | _                     |  |
| maleic anhydride                     | $C_4H_2O_3$                     | 99.008                | -9%                      | -10%                | $C_4H_4O_4H^+$                     | 117.018        | 7 %-31 %              |  |

midity proxy varied from 0.2% to 8% by vaporizing water into the calibration gas stream (Sect. 2). Figure 3 shows that sensitivities for all five furanoid are minimally impacted by humidity within this range, with the sensitivity change generally within the calibration uncertainty of 10%. 2(3H)-furanone sensitivity was the least impacted by humidity, changing by less than 1%. Furan, 2-furaldehyde, 2,5-dimethylfuran, and maleic anhydride sensitivities change by 6%–15%, with furan and maleic anhydride sensitivities be-

ing negatively correlated with humidity while 2-furaldehyde and 2,5-dimethlyfuran are positively correlated.

Figure 4 shows how the sensitivities for the five furanoids are impacted by changing the instrument E/N from 110–150 Td at a narrow fixed m39 / m21 range. Furan sensitivity is least dependent on E/N, decreasing by 2% over the range investigated. This is consistent with it not having any major fragmentation (Fig. 2). Alternatively, 2(3H)-furanone, 2-furaldehyde, 2,5-dimethylfuran, and maleic anhydride sensitivities all decrease 5%–10% with higher E/N. For 2(3H)-

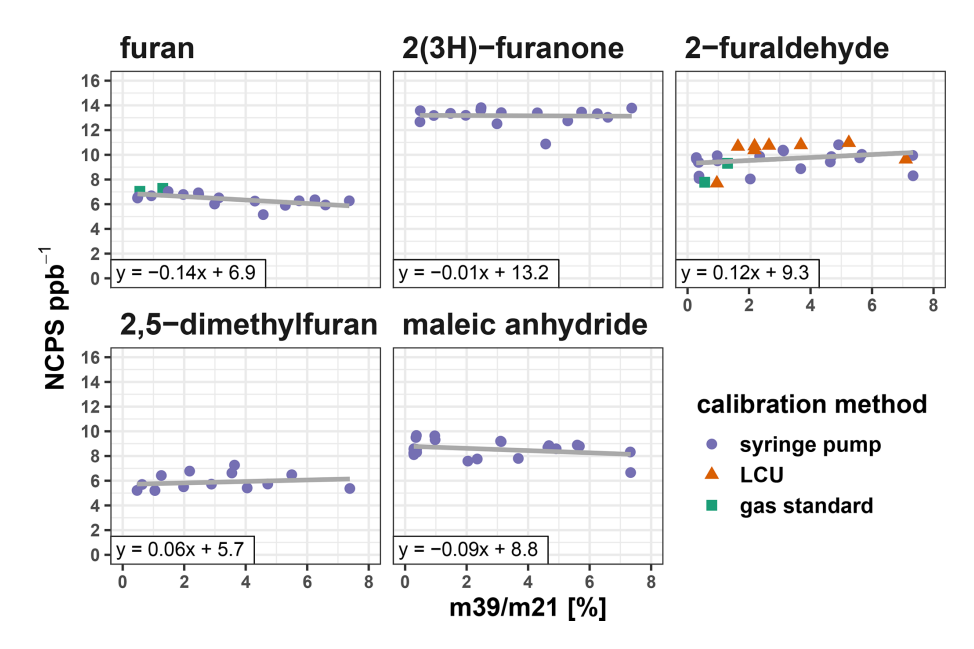


**Figure 3.** PTR-MS instrument sensitivity (expressed as normalized counts per second per ppb) as a function of humidity in the drift tube (expressed as mass 39/mass 21 humidity proxy). When available, different calibration methods are colored corresponding to those done using compressed gas standard cylinders, Liquid Calibration Unit, or syringe pump.

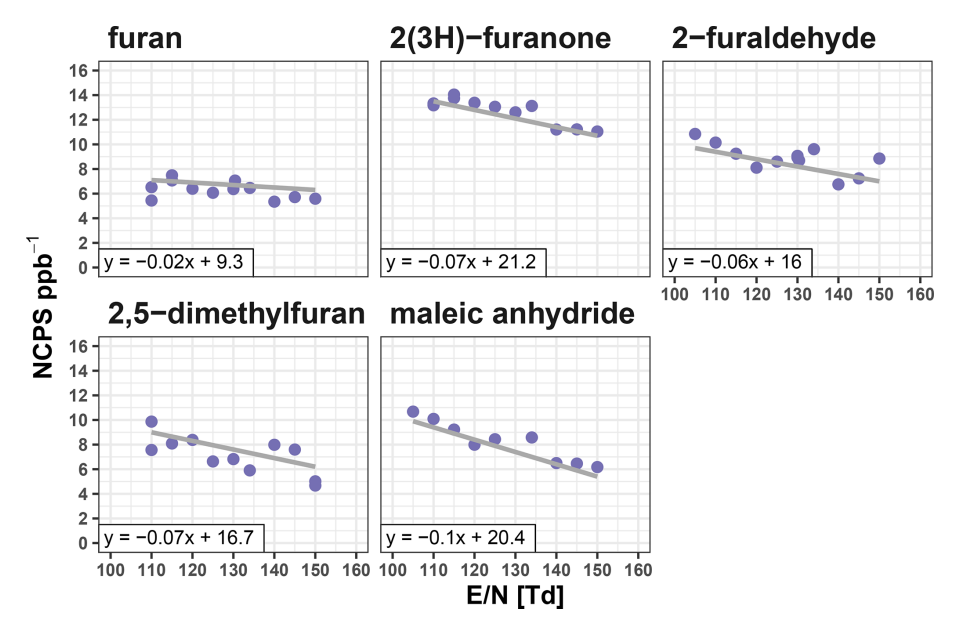


**Figure 4.** Instrument sensitivity for furan, 2(3H)-furanone, furaldehyde, 2,5-dimethylfuran, and maleic anhydride as a product of the drift tube electric field strength (E/N) from 110–150 Td.

furanone, 2-furaldehyde, and maleic anhydride this likely reflects the increased prevalence of the hydrated ion and fragmentation at higher E/N. Additionally, it is likely these furanoids are reactive with the  $\rm H_2O(H_3O)^+$  cluster (proton affinity 801 kJ mol<sup>-1</sup>, Yuan et al., 2016), which is more favorable at lower E/N conditions. Overall, the E/N has a minimal impact on the sensitivity of these five furanoids, with the variability again within the calibration uncertainty. However, it is

notable that higher E/N may negatively affect the quantification of masses with interfering fragments from these species.

## 3.3 Stability of gas standard concentrations and their instrument sensitivities'

The recertification of two compressed gas cylinders (Apel-Riemer Environmental, Inc.) show that the mixing ratios in the tanks changed by less than 1% in the seven years since

**Table 2.** Comparisons of long-term sensitivities and gas standard concentrations for the furanoids discussed in this work. Data from 2017 corresponds to when the PTR-ToF-MS and gas standard was new. Data from 2024 is after seven years of use and corresponds with the gas standard being recertified. Calculated sensitivities follow Sekimoto et al. (2017) using 2024 sensitivities, and are shown with their percent difference of 2024 calibrations factors. Note that empty values correspond to sensitivities for species that are not present in the gas standards.

|                   |      | s standa<br>ntration |       | Sensitivity [NCPS/ppb] |      |       | Sensitivity calculated<br>per Sekimoto et al.<br>(2017) (% diff.) |
|-------------------|------|----------------------|-------|------------------------|------|-------|---|
| Species           | 2017 | 2024                 | diff. | 2017                   | 2024 | diff. |   |
| furan             | 1022 | 1029                 | 1 %   | 10.9                   | 6.7  | -39 % | 5.8 (-13%)  |
| 2-methylfuran     | 978  | 1009                 | 3 %   | 10.9                   | 7.4  | -32%  | 6.3 (-15%)  |
| 2-(3H)furanone    | _    | _                    | _     | _                      | 13.1 | _     | 7.5 (-42%)  |
| 2-furaldehyde     | 1000 | 1003                 | 0%    | 16.2                   | 9.5  | -41%  | 12.3 (30 %)   |
| 2,5-dimethylfuran | _    | _                    | _     | _                      | 5.9  | _     | 6.8 (16 %)  |
| maleic anhydride  | _    | _                    | _     | _                      | 8.7  | _     | 9.8 (13 %)  |
| 5-methylfurfural  | 977  | 999                  | 2 %   | 17.2                   | 6.9  | -60%  | 11.1 (61 %)   |

the standards were made (Furanoids summarized in Table 2 with the remaining VOCs in Table A1). For all VOCs, the change is well within the uncertainty of the recertification analysis  $(\pm 5\,\%)$  and demonstrates that these furanoids and other VOCs are remarkably stable in gas standards.

Table 2 also shows how the sensitivity of our PTR-ToF-MS has changed over those same seven years, with the sensitivities for the four furanoids in our gas standard decreasing from 32 %-60 %. This decrease in sensitivity is also present in the other species regularly calibrated using gas standards (Table A1). Given that mixing ratios for all species in the gas standards have changed less than 5 % over this period, the decreased instrument sensitivity likely reflects a wearing of the instrument; with sensitivity being especially high in the new factory-tuned instrument then leveling out as the electronics aged. This seven-year period also corresponds with the lifetime of the microchannel plate (MCP) detector in this particular instrument, which was replaced shortly after the calibrations in this study. Although the exact mechanisms leading to a systematic drift in instrument sensitivity are beyond the scope of this work, it reiterates the importance of performing calibrations during field deployments and revisiting them over an instrument's lifetime.

Detailed laboratory calibrations are often time-consuming and impractical to obtain for the hundreds of different VOCs measured by PTR-ToF-MS. However, one major benefit of PTR-MS is that sensitivities can be readily calculated using known drift tube parameters (i.e., pressure, temperature, voltage, and length) and each VOC's proton transfer reaction rate with  $\rm H_3O^+$  ( $k_{\rm PTR}$ ) (de Gouw and Warneke, 2007). A notable limitation of this approach is that well defined  $k_{\rm PTR}$  values are needed for each VOC of interest, which is often not the case for newly identified species, including all furnaoids in this work except furan and 2-furaldehyde.

In the absence of known  $k_{PTR}$  values, Sekimoto et al. (2017) showed that proton transfer reaction rates could be es-

timated using molecular properties ( $k_{\rm cap}$ ). As  $k_{\rm PTR}$  has a linear relationship with instrument sensitivity (Cappellin et al., 2012; Sekimoto et al., 2017), the slope of the regression between  $k_{\rm PTR}$ , and by extension  $k_{\rm cap}$ , versus sensitivities measured from direct calibration can then be used to calculate sensitivities for unknown VOCs. For the instrument used in this work, the slope of  $k_{\rm cap}$  vs. sensitivity is  $3.3 \times 10^9$  with an  $r^2$  of 0.93. The accuracy of this approach is estimated to be less than 50%, determined by the difference between the estimated sensitivities and the calibrated ones for selected VOCs (Permar et al., 2021; Sekimoto et al., 2017; Selimovic et al., 2022).

Table 2 shows how the furanoid sensitivities from calibrations in this work compare to those calculated based on the method described by Sekimoto et al. (2017). Table A1 shows the same for the other 21 VOCs in our gas standards. For the furanoids reported here, we find that direct calibrations for all furanoids except 5-methylfurfural agree within less than 42 % of those calculated from their molecular properties. The reason for 5-methylfurfural's calculated sensitivity being 60 % lower than its measured is unknown, though it could in part be due to reaction with the water dimer which is not accounted for in these calculations. This indicates that in the absence of direct furanoid calibrations, their kinetically calculated sensitivities provide a good estimate of the instrument response. We also find that the slope of the correlation between  $k_{cap}$  and the measured sensitivities for 25 directly calibrated VOCs decreased by 33 % in the seven years from 2017 to 2024, representative of the overall decrease in instrument sensitivity described above. Consequently, calibration factors calculated based on the correlation of  $k_{PTR}$  vs. sensitivity of directly calibrated species should also be revisited regularly to account for changes in instrument response.

**Table 3.** Potential interfering isomers in fresh BB smoke for furanoid masses discussed in this work. Known isomers that have been reported in BB smoke are listed, though most are from studies without co-deployed PTR-MS. Fractional contributions are for each isomer to the total PTR-ToF-MS signal at that mass where available. Values from Koss et al. (2018) are from laboratory burning experiments and a combination of online GC-MS measurements, literature review, and correlation analysis. Fractions for Permar et al. (2021) and Gkatzelis et al. (2024) represent wildfire emissions measured by aircraft 10–120 min downwind from the fire and are calculated from co-deployed GC-MS measurements made by TOGA. Unidentified fractional contributions represent the remaining portion of the instrument signal not attributed to the corresponding known isomers at that mass.

|                |  |  | Fracti                            | onal contribution in             | smoke                            |  |
|----------------|--|--|-----------------------------------|----------------------------------|----------------------------------|--|
| Ion mass $m/z$ | Formula                                      | Isomers known to be in BB smoke from largest to smallest contribution  | Koss et al. (2017)                | Gkatzelis et al. (2024)          | Permar et al. (2021)             |  |
| 69.033         | C <sub>4</sub> H <sub>4</sub> O              | furan <sup>2–4,7,11,12,19,21</sup>   | 100 % <sup>23</sup>               | 46 %                             | 66 %                             |  |
| 83.049         | C <sub>5</sub> H <sub>6</sub> O              | 2-methylfuran <sup>2</sup> –4,6,9,11,12,18,19,21,22 3-Methylfuran <sup>4</sup> ,6,11,12 cyclopentenones <sup>4</sup> ,6 Likely minor: Pent-2-ynal <sup>6</sup> 1,4-Pentadien-3-one <sup>6</sup>                    | 51 %<br>10 %<br>37 % unidentified | 15 %<br>3 %<br>82 % unidentified | 16 %<br>3 %<br>81 % unidentified |  |
| 85.028         | $C_4H_4O_2$                                  | 2-(3H)furanone <sup>1,2,8,12,14,17,19</sup>  |                                   |                                  |                                  |  |
| 97.028         | C <sub>5</sub> H <sub>4</sub> O <sub>2</sub> | 2-furaldehyde <sup>1,4,6,8,9,12–14,18,19</sup> 3-Furaldehyde <sup>2,4,6,11,12,19,21</sup> cyclopentenediones <sup>4,6,22</sup>   | 84 %<br>4 %<br>11 % unidentified  | 22 %<br>2 %<br>76 % unidentified |                                  |  |
| 97.065         | C <sub>6</sub> H <sub>8</sub> O              | 2,5-dimethylfuran <sup>2</sup> –4,6,11,12,18,19,22<br>2-Ethylfuran <sup>2</sup> ,4,6,11,19,22<br>2-Methylcyclopentenone <sup>7</sup> ,13,14,17<br>2,4-dimethylfuran <sup>6</sup><br>2,3-dimethylfuran <sup>6</sup> | 44 %<br>10 %<br>46 % unidentified |                                  |                                  |  |
| 99.008         | C <sub>4</sub> H <sub>2</sub> O <sub>3</sub> | maleic anhydride <sup>3,15</sup>   |                                   |                                  |                                  |  |
| 111.044        | C <sub>6</sub> H <sub>6</sub> O <sub>2</sub> | 5-methylfurfural <sup>3,6,10,12,14,17–19</sup> Catechol (Benzenediols) <sup>3,4,8,12,13,17–20</sup> 2-acetylfuran <sup>6</sup>   | 5                                 |                                  |                                  |  |

References: <sup>1</sup> Azeez et al. (2011). <sup>2</sup> Brilli et al. (2014). <sup>3</sup> Bruns et al. (2017). <sup>4</sup> Gilman et al. (2015). <sup>5</sup> Gkatzelis et al. (2024). <sup>6</sup> Hatch et al. (2015). <sup>7</sup> Hatch et al. (2019). <sup>8</sup> Heigenmoser et al. (2013). <sup>9</sup> Ingemarsson et al. (1998). <sup>10</sup> Jordan and Seen (2005). <sup>11</sup> Karl et al. (2007). <sup>12</sup> Koss et al. (2017). <sup>13</sup> Li et al. (2013). <sup>14</sup> Liu et al. (2012). <sup>15</sup> Müller et al. (2016). <sup>16</sup> Permar et al. (2021). <sup>17</sup> Pittman et al. (2012). <sup>18</sup> Simmleit and Schulten (1989). <sup>19</sup> Stockwell et al. (2015). <sup>20</sup> Veres et al. (2010). <sup>21</sup> Warneke et al. (2011b). <sup>22</sup> Yokelson et al. (2013). <sup>23</sup> From eight laboratory burns, four of which the GC shows many small peaks with furan being less than 3% of the signal, while the other four attribute the full signal to furan.

### 3.4 Furanoid speciation and potential fragment interference in PTR-ToF-MS

The lack of major fragmentation and humidity dependence as described above demonstrates that PTR-ToF-MS furanoid measurements are robust under standard sampling conditions. Additionally, the long-term stability of key furanoids in calibration standards means that instrument sensitivities should be well quantified with regular calibrations. Consequently, the discrepancy between PTR-ToF-MS and GC-MS furanoid measurements in BB smoke cannot be explained by calibration error alone and is instead likely due to the presence of unidentified interfering fragments and/or isomers. Extensive work has been done to identify PTR-ToF-MS measured masses in BB smoke, relying on both direct speciated

measurements and association with compounds known to be in smoke from literature review.

Table 3 shows potential interfering isomers in BB smoke for the furanoid masses calibrated here, as well as three others we regularly calibrate via their gas standards. Importantly, although each of these isomers have been reported to be present in BB smoke, little work has been done to determine their fractional contributions. Additionally, the extent of interference from fragments of high order masses is largely unknown. This is due to the difficulty in making such speciated measurements in complex airmasses, where PTR-ToF-MS measurements would need to be done in-line with a separation technique such as gas chromatography.

For fresh BB emissions, one of the most complete studies reporting speciated furanoid measurements from PTR-ToF-

MS was done by Koss et al. (2018) using laboratory burning experiments and a combination of online GC-MS measurements, literature review, and correlation analysis. In Table 3 we report the fractional distribution for each of the masses calibrated in this work as reported by Koss et al. (2018). Additional fractional speciation is reported from Permar et al. (2021) and Gkatzelis et al. (2024) where available. We note that the fractional contributions from Koss et al. (2018) are based on very fresh smoke measured directly above a laboratory burn, while those from Permar et al. (2021) and Gkatzelis et al. (2024) represent wildfire emissions measured by aircraft 10–120 min downwind from the fire and calculated from co-deployed GC-MS measurements made by TOGA (Apel et al., 2003, 2010, 2015; Hornbrook et al., 2011).

As demonstrated in Table 3 and by measurement comparisons between PTR-ToF-MS and GC-MS, large discrepancies exist in the speciation of masses attributed to furan, methyl furans, and furaldehydes in BB smoke. For example, m/z 69.033 is attributed to just furan in very fresh laboratory BB emissions, while only 46%–66% is attributed as furan in wildfire plumes sampled 20–120 min down wind of their source. Similarly, methyl furans at m/z 83.049 and furaldehydes at m/z 97.065 also have a higher unknown fraction in the field measurements. This may be due to the rapid change in smoke composition as it ages post emission, with unidentified isomers or fragments being formed.

This variability highlights that as BB plumes age, isomers and fragments can significantly contribute to the signals of some furanoids. Such processes complicate PTR-ToF-MS interpretation of these masses in aged smoke, urban environments, and mixed smoke/urban air masses where little to no detailed speciation has been done. While laboratory and field studies suggest that furanoids are reliable BB tracers, in the absence of complimentary measurements, their accuracy in aged smoke may be less robust. Consequently, more detailed studies utilizing co-deployed GC and PTR-MS are needed to better measure furanoids in varying real-world conditions.

#### 4 Conclusions

Detailed laboratory characterization of furan (C<sub>4</sub>H<sub>4</sub>O, m/z 69.033), 2(3H)-furanone (C<sub>4</sub>H<sub>4</sub>O<sub>2</sub>, m/z 85.028), 2-furaldehyde (C<sub>5</sub>H<sub>4</sub>O<sub>2</sub>, m/z 97.028), 2,5-dimethylfuran (C<sub>6</sub>H<sub>8</sub>O, m/z 97.065), and maleic anhydride (C<sub>4</sub>H<sub>2</sub>O<sub>3</sub>, m/z 99.008) demonstrates that their sensitivities in PTR-ToF-MS have minimal humidity and drift tube electric field strength (E/N) dependence (< 15%). Furan and 2,5-dimethylfuran were found to not fragment upon proton transfer reaction. However, 2-furaldehyde was found to fragment at ~8%, under typical operation conditions (E/N 130 Td), to m/z 69.033, interfering with the measurement of furan. A hydrolysis product was also observed for 2(3H)-furanone, 2-furaldehyde, and maleic anhydride, corresponding to their

m/z +18 ion mass. For 2(3H)-furanone, 2-furaldehyde this product is minor, accounting for < 7% of their parent mass at E/N 150 Td. The hydrolysis of maleic anhydride to maleic acid is more favorable, ranging from 7%–31% of the parent ion signal over the E/N range of 110–150 Td. Although we do not directly calibrate succinic anhydride in this work, we hypothesize that it will also undergo a similar hydration reaction as maleic anhydride in the PTR-MS.

Recertification of seven-year-old gas standard mixtures also showed that furanoids and other VOCs are very stable in compressed gas cylinders, with most mixing ratios changing by less than 1 % over the period. Over the same period average instrument sensitivities for the PTR-ToF-MS used in this work were found to decrease by  $\sim 33\,\%$ . This likely represents a settling in of the instrument electronics from its factory new condition, along with the aging of the MCP.

The stability of the furanoid gas standards, coupled with the minimal fragmentation and humidity dependence indicates that with regular calibrations PTR-ToF-MS measures furanoids accurately. Despite this, mixing ratios reported by PTR-ToF-MS measurements have been found to be significantly higher than those made by co-deployed GC-MS, indicating the presence of interfering isomers and/or fragments in PTR-ToF-MS. The full extent of these interferences is currently difficult to quantify because their contributions cannot be fully resolved without chromatographic separation, which decreases temporal resolution while adding instrument and analysis complexity. Consequently, improving the accuracy of furanoid measurements made by PTR-MS will require codeployed GC-MS and/or GC-PTR-ToF-MS configurations to identify fragment and isomer interferences in complex air mixtures, including aged BB smoke and urban environments.

#### Appendix A

**Table A1.** Comparisons of long-term sensitivities and gas standard concentrations for 21 additional VOCs discussed in this work. Data from 2017 corresponds to when the PTR-ToF-MS and gas standards were new. Data from 2024 is after seven years of use and corresponds with the gas standards being recertified. Calculated sensitivities follow Sekimoto et al. (2017) using 2024 sensitivities and are shown with their percent difference of 2024 calibrations factors.

|                            | Gas standard concentration [ppb] |      |       | Sensitivity [NCPS/ppb] |      |              | Sensitivity calculated per Sekimoto et al. (2017) (% diff.) |
|----------------------------|----------------------------------|------|-------|------------------------|------|--------------|---|
| Species                    | 2017                             | 2024 | diff. | 2017                   | 2024 | diff.        |   |
| Methanol                   | 1022                             | 1010 | -1%   | 16.3                   | 10.6 | <b>-35</b> % | 7.4 (-30%)  |
| Propyne                    | 1007                             | 993  | -1%   | 9.4                    | 7.1  | -24%         | 5.4 (-25%)  |
| Acetonitrile               | 1016                             | 1024 | 1 %   | 21.6                   | 15.0 | -30%         | 12.8 (-15%)   |
| Acetaldehyde               | 1022                             | 995  | -3%   | 18.9                   | 12.5 | -34%         | 10.0(-20%)  |
| Ethanol                    | 1019                             | 1032 | 1 %   | 0.9                    | 0.7  | -26%         | 7.4 (999 %)   |
| 1-butene                   | 1003                             | 999  | 0%    | 6.2                    | 4.3  | -30%         | 5.8 (34 %)  |
| Acetone                    | 972                              | 977  | 1 %   | 20.1                   | 14.9 | -26%         | 10.4 (-30%)   |
| Dimethyl sulfide           | 1000                             | 992  | -1%   | 12                     | 9.2  | -24%         | 6.9(-24%)   |
| Isoprene                   | 989                              | 982  | -1%   | 7.3                    | 4.8  | -34%         | 6.3 (32 %)  |
| Methyl vinyl ketone        | 971                              | 993  | 2 %   | 15.9                   | 10.1 | -36%         | 10.6 (5 %)  |
| Methacrolein               | 1007                             | 996  | -1%   | 11.1                   | 7.3  | -34%         | 10.6 (45 %)   |
| Methyl ethyl ketone        | 1011                             | 1049 | 4 %   | 18.1                   | 12.1 | -33%         | 10.3 (-15%)   |
| Benzene                    | 999                              | 1006 | 1 %   | 9.4                    | 6.9  | -26%         | 6.4 (-8%)   |
| Toluene                    | 994                              | 1002 | 1 %   | 10.6                   | 7.3  | -31%         | 6.8 (-7%)   |
| 3-hexanone                 | 943                              | 941  | 0%    | 13.5                   | 7.6  | -44%         | 10.4 (36 %)   |
| Ethylbenzene               | 1003                             | 995  | -1%   | 5.3                    | 3.4  | -36%         | 7.3 (115 %)   |
| <i>m</i> -xylene           | 990                              | 975  | -2%   | 9.5                    | 6.7  | -30%         | 7.3 (10%)   |
| 1,2,4-trimethylbenzene     | 999                              | 988  | -1%   | 11.3                   | 6.4  | -44%         | 7.6 (19 %)  |
| 1,3,5-trimethylbenzene     | 989                              | 988  | 0%    | 11.3                   | 7.1  | -37%         | 7.6 (7 %)   |
| 1,2,3,5-tetramethylbenzene | 997                              | 997  | 0%    | 11.5                   | 6.9  | -40%         | 8.0 (16 %)  |
| $\alpha$ -pinene           | 967                              | 954  | -1%   | 5.1                    | 2.8  | -45%         | 8.1 (186%)  |

*Code availability.* The code related to this article is available upon request to the corresponding author.

Data availability. The data related to this article is available upon request to the corresponding author.

Author contributions. WP: conceptualization, methodology, investigation, data curation, formal analysis, and original draft preparation. MT: investigation, methodology, review and editing. LH: conceptualization, funding acquisition, supervision, review and editing.

Competing interests. The contact author has declared that none of the authors has any competing interests.

*Disclaimer.* Publisher's note: Copernicus Publications remains neutral with regard to jurisdictional claims made in the text, published maps, institutional affiliations, or any other geographical rep-

resentation in this paper. While Copernicus Publications makes every effort to include appropriate place names, the final responsibility lies with the authors. Views expressed in the text are those of the authors and do not necessarily reflect the views of the publisher.

Acknowledgements. The authors acknowledge the use of OpenAI's ChatGPT for assistance with light editing, including writing clarity, grammar, and summarization during the preparation of this manuscript. All results, analysis, and interpretations are solely those of the authors.

*Financial support.* This research has been supported by the National Science Foundation (grant nos. AGS-2144896 and EPSCoR-2242802).

*Review statement.* This paper was edited by Bin Yuan and reviewed by two anonymous referees.

#### References

- Akagi, S. K., Yokelson, R. J., Wiedinmyer, C., Alvarado, M. J., Reid, J. S., Karl, T., Crounse, J. D., and Wennberg, P. O.: Emission factors for open and domestic biomass burning for use in atmospheric models, Atmos. Chem. Phys., 11, 4039–4072, https://doi.org/10.5194/acp-11-4039-2011, 2011.
- Apel, E. C., Hills, A. J., Lueb, R., Zindel, S., Eisele, S., and Riemer, D. D.: A fast-GC/MS system to measure C2 to C4 carbonyls and methanol aboard aircraft, Journal of Geophysical Research: Atmospheres, 108, 8794, https://doi.org/10.1029/2002JD003199, 2003.
- Apel, E. C., Emmons, L. K., Karl, T., Flocke, F., Hills, A. J., Madronich, S., Lee-Taylor, J., Fried, A., Weibring, P., Walega, J., Richter, D., Tie, X., Mauldin, L., Campos, T., Weinheimer, A., Knapp, D., Sive, B., Kleinman, L., Springston, S., Zaveri, R., Ortega, J., Voss, P., Blake, D., Baker, A., Warneke, C., Welsh-Bon, D., de Gouw, J., Zheng, J., Zhang, R., Rudolph, J., Junkermann, W., and Riemer, D. D.: Chemical evolution of volatile organic compounds in the outflow of the Mexico City Metropolitan area, Atmos. Chem. Phys., 10, 2353–2375, https://doi.org/10.5194/acp-10-2353-2010, 2010.
- Apel, E. C., Hornbrook, R. S., Hills, A. J., Blake, N. J., Barth, M. C., Weinheimer, A., Cantrell, C., Rutledge, S. A., Basarab, B., Crawford, J., Diskin, G., Homeyer, C. R., Campos, T., Flocke, F., Fried, A., Blake, D. R., Brune, W., Pollack, I., Peischl, J., Ryerson, T., Wennberg, P. O., Crounse, J. D., Wisthaler, A., Mikoviny, T., Huey, G., Heikes, B., O'Sullivan, D., and Riemer, D. D.: Upper tropospheric ozone production from lightning NOx-impacted convection: Smoke ingestion case study from the DC3 campaign, Journal of Geophysical Research: Atmospheres, 120, 2505–2523, https://doi.org/10.1002/2014JD022121, 2015.
- Azeez, A. M., Meier, D., and Odermatt, J.: Temperature dependence of fast pyrolysis volatile products from European and African biomasses, Journal of Analytical and Applied Pyrolysis, 90, 81– 92, https://doi.org/10.1016/j.jaap.2010.11.005, 2011.
- Baasandorj, M., Millet, D. B., Hu, L., Mitroo, D., and Williams, B. J.: Measuring acetic and formic acid by proton-transferreaction mass spectrometry: sensitivity, humidity dependence, and quantifying interferences, Atmos. Meas. Tech., 8, 1303– 1321, https://doi.org/10.5194/amt-8-1303-2015, 2015.
- Brilli, F., Gioli, B., Ciccioli, P., Zona, D., Loreto, F., Janssens, I. A., and Ceulemans, R.: Proton Transfer Reaction Time-of-Flight Mass Spectrometric (PTR-TOF-MS) determination of volatile organic compounds (VOCs) emitted from a biomass fire developed under stable nocturnal conditions, Atmospheric Environment, 97, 54–67, https://doi.org/10.1016/j.atmosenv.2014.08.007, 2014.
- Bruns, E. A., Slowik, J. G., El Haddad, I., Kilic, D., Klein, F., Dommen, J., Temime-Roussel, B., Marchand, N., Baltensperger, U., and Prévôt, A. S. H.: Characterization of gas-phase organics using proton transfer reaction time-of-flight mass spectrometry: fresh and aged residential wood combustion emissions, Atmos. Chem. Phys., 17, 705–720, https://doi.org/10.5194/acp-17-705-2017, 2017.
- Cappellin, L., Karl, T., Probst, M., Ismailova, O., Winkler, P. M., Soukoulis, C., Aprea, E., Märk, T. D., Gasperi, F., and Biasioli, F.: On Quantitative Determination of Volatile Organic Compound Concentrations Using Proton Transfer Reaction Time-of-

- Flight Mass Spectrometry, Environ. Sci. Technol., 46, 2283–2290, https://doi.org/10.1021/es203985t, 2012.
- Coggon, M. M., Lim, C. Y., Koss, A. R., Sekimoto, K., Yuan, B., Gilman, J. B., Hagan, D. H., Selimovic, V., Zarzana, K. J., Brown, S. S., Roberts, J. M., Müller, M., Yokelson, R., Wisthaler, A., Krechmer, J. E., Jimenez, J. L., Cappa, C., Kroll, J. H., de Gouw, J., and Warneke, C.: OH chemistry of non-methane organic gases (NMOGs) emitted from laboratory and ambient biomass burning smoke: evaluating the influence of furans and oxygenated aromatics on ozone and secondary NMOG formation, Atmos. Chem. Phys., 19, 14875–14899, https://doi.org/10.5194/acp-19-14875-2019, 2019.
- Coggon, M. M., Stockwell, C. E., Claflin, M. S., Pfannerstill, E. Y., Xu, L., Gilman, J. B., Marcantonio, J., Cao, C., Bates, K., Gkatzelis, G. I., Lamplugh, A., Katz, E. F., Arata, C., Apel, E. C., Hornbrook, R. S., Piel, F., Majluf, F., Blake, D. R., Wisthaler, A., Canagaratna, M., Lerner, B. M., Goldstein, A. H., Mak, J. E., and Warneke, C.: Identifying and correcting interferences to PTR-ToF-MS measurements of isoprene and other urban volatile organic compounds, Atmos. Meas. Tech., 17, 801–825, https://doi.org/10.5194/amt-17-801-2024, 2024.
- Cope, E. M., Ketcherside, D. T., Jin, L., Tan, L., Mansfield, M., Jones, C., Lyman, S., Jaffe, D., and Hu, L.: Sources of Atmospheric Volatile Organic Compounds During the Salt Lake Regional Smoke, Ozone and Aerosol Study (SAMOZA) 2022, Journal of Geophysical Research: Atmospheres, 129, e2024JD041640, https://doi.org/10.1029/2024JD041640, 2024.
- Crews, C. and Castle, L.: A review of the occurrence, formation and analysis of furan in heat-processed foods, Trends in Food Science & Technology, 18, 365–372, https://doi.org/10.1016/j.tifs.2007.03.006, 2007.
- de Gouw, J. A. and Warneke, C.: Measurements of volatile organic compounds in the earth's atmosphere using proton-transferreaction mass spectrometry, Mass Spectrom. Rev., 26, 223–257, https://doi.org/10.1002/mas.20119, 2007.
- Gilman, J. B., Lerner, B. M., Kuster, W. C., Goldan, P. D., Warneke, C., Veres, P. R., Roberts, J. M., de Gouw, J. A., Burling, I. R., and Yokelson, R. J.: Biomass burning emissions and potential air quality impacts of volatile organic compounds and other trace gases from fuels common in the US, Atmos. Chem. Phys., 15, 13915–13938, https://doi.org/10.5194/acp-15-13915-2015, 2015.
- Gkatzelis, G. I., Coggon, M. M., Stockwell, C. E., Hornbrook, R. S., Allen, H., Apel, E. C., Bela, M. M., Blake, D. R., Bourgeois, I., Brown, S. S., Campuzano-Jost, P., St. Clair, J. M., Crawford, J. H., Crounse, J. D., Day, D. A., DiGangi, J. P., Diskin, G. S., Fried, A., Gilman, J. B., Guo, H., Hair, J. W., Halliday, H. S., Hanisco, T. F., Hannun, R., Hills, A., Huey, L. G., Jimenez, J. L., Katich, J. M., Lamplugh, A., Lee, Y. R., Liao, J., Lindaas, J., Mc-Keen, S. A., Mikoviny, T., Nault, B. A., Neuman, J. A., Nowak, J. B., Pagonis, D., Peischl, J., Perring, A. E., Piel, F., Rickly, P. S., Robinson, M. A., Rollins, A. W., Ryerson, T. B., Schueneman, M. K., Schwantes, R. H., Schwarz, J. P., Sekimoto, K., Selimovic, V., Shingler, T., Tanner, D. J., Tomsche, L., Vasquez, K. T., Veres, P. R., Washenfelder, R., Weibring, P., Wennberg, P. O., Wisthaler, A., Wolfe, G. M., Womack, C. C., Xu, L., Ball, K., Yokelson, R. J., and Warneke, C.: Parameterizations of US wildfire and prescribed fire emission ratios and emission factors based

- on FIREX-AQ aircraft measurements, Atmos. Chem. Phys., 24, 929–956, https://doi.org/10.5194/acp-24-929-2024, 2024.
- Hatch, L. E., Luo, W., Pankow, J. F., Yokelson, R. J., Stockwell, C. E., and Barsanti, K. C.: Identification and quantification of gaseous organic compounds emitted from biomass burning using two-dimensional gas chromatography-time-of-flight mass spectrometry, Atmos. Chem. Phys., 15, 1865–1899, https://doi.org/10.5194/acp-15-1865-2015, 2015.
- Hatch, L. E., Jen, C. N., Kreisberg, N. M., Selimovic, V., Yokelson, R. J., Stamatis, C., York, R. A., Foster, D., Stephens, S. L., Goldstein, A. H., and Barsanti, K. C.: Highly Speciated Measurements of Terpenoids Emitted from Laboratory and Mixed-Conifer Forest Prescribed Fires, Environ. Sci. Technol., 53, 9418–9428, https://doi.org/10.1021/acs.est.9b02612, 2019.
- Heigenmoser, A., Liebner, F., Windeisen, E., and Richter, K.: Investigation of thermally treated beech (*Fagus sylvatica*) and spruce (*Picea abies*) by means of multifunctional analytical pyrolysis-GC/MS, Journal of Analytical and Applied Pyrolysis, 100, 117–126, https://doi.org/10.1016/j.jaap.2012.12.005, 2013.
- Hornbrook, R. S., Blake, D. R., Diskin, G. S., Fried, A., Fuelberg, H. E., Meinardi, S., Mikoviny, T., Richter, D., Sachse, G. W., Vay, S. A., Walega, J., Weibring, P., Weinheimer, A. J., Wiedinmyer, C., Wisthaler, A., Hills, A., Riemer, D. D., and Apel, E. C.: Observations of nonmethane organic compounds during ARCTAS Part 1: Biomass burning emissions and plume enhancements, Atmos. Chem. Phys., 11, 11103–11130, https://doi.org/10.5194/acp-11-11103-2011, 2011.
- Huangfu, Y., Yuan, B., Wang, S., Wu, C., He, X., Qi, J., de Gouw, J., Warneke, C., Gilman, J. B., Wisthaler, A., Karl, T., Graus, M., Jobson, B. T., and Shao, M.: Revisiting Acetonitrile as Tracer of Biomass Burning in Anthropogenic-Influenced Environments, Geophysical Research Letters, 48, e2020GL092322, https://doi.org/10.1029/2020GL092322, 2021.
- Ingemarsson, Å., Nilsson, U., Nilsson, M., Pedersen, J. R., and Olsson, J. O.: Slow pyrolysis of spruce and pine samples studied with GC/MS and GC/FTIR/FID, Chemosphere, 36, 2879–2889, https://doi.org/10.1016/S0045-6535(97)10245-4, 1998.
- Joo, T., Rivera-Rios, J. C., Takeuchi, M., Alvarado, M. J., and Ng, N. L.: Secondary Organic Aerosol Formation from Reaction of 3-Methylfuran with Nitrate Radicals, ACS Earth Space Chem., 3, 922–934, https://doi.org/10.1021/acsearthspacechem.9b00068, 2019.
- Jordan, T. B. and Seen, A. J.: Effect of Airflow Setting on the Organic Composition of Woodheater Emissions, Environ. Sci. Technol., 39, 3601–3610, https://doi.org/10.1021/es0487628, 2005.
- Karl, T. G., Christian, T. J., Yokelson, R. J., Artaxo, P., Hao, W. M., and Guenther, A.: The Tropical Forest and Fire Emissions Experiment: method evaluation of volatile organic compound emissions measured by PTR-MS, FTIR, and GC from tropical biomass burning, Atmos. Chem. Phys., 7, 5883–5897, https://doi.org/10.5194/acp-7-5883-2007, 2007.
- Koss, A., Yuan, B., Warneke, C., Gilman, J. B., Lerner, B. M.,
  Veres, P. R., Peischl, J., Eilerman, S., Wild, R., Brown, S. S.,
  Thompson, C. R., Ryerson, T., Hanisco, T., Wolfe, G. M., Clair,
  J. M. St., Thayer, M., Keutsch, F. N., Murphy, S., and de Gouw,
  J.: Observations of VOC emissions and photochemical products
  over US oil- and gas-producing regions using high-resolution

- H<sub>3</sub>O<sup>+</sup> CIMS (PTR-ToF-MS), Atmos. Meas. Tech., 10, 2941–2968, https://doi.org/10.5194/amt-10-2941-2017, 2017.
- Koss, A. R., Sekimoto, K., Gilman, J. B., Selimovic, V., Coggon, M. M., Zarzana, K. J., Yuan, B., Lerner, B. M., Brown, S. S., Jimenez, J. L., Krechmer, J., Roberts, J. M., Warneke, C., Yokelson, R. J., and de Gouw, J.: Non-methane organic gas emissions from biomass burning: identification, quantification, and emission factors from PTR-ToF during the FIREX 2016 laboratory experiment, Atmos. Chem. Phys., 18, 3299–3319, https://doi.org/10.5194/acp-18-3299-2018, 2018.
- Li, Q., Steele, P. H., Yu, F., Mitchell, B., and Hassan, E.-B. M.: Pyrolytic spray increases levoglucosan production during fast pyrolysis, Journal of Analytical and Applied Pyrolysis, 100, 33–40, https://doi.org/10.1016/j.jaap.2012.11.013, 2013.
- Liang, Y., Weber, R. J., Misztal, P. K., Jen, C. N., and Goldstein,
  A. H.: Aging of Volatile Organic Compounds in October 2017
  Northern California Wildfire Plumes, Environ. Sci. Technol., 56,
  1557–1567, https://doi.org/10.1021/acs.est.1c05684, 2022.
- Liu, Y., Shi, Q., Zhang, Y., He, Y., Chung, K. H., Zhao, S., and Xu, C.: Characterization of Red Pine Pyrolysis Bio-oil by Gas Chromatography–Mass Spectrometry and Negative-Ion Electrospray Ionization Fourier Transform Ion Cyclotron Resonance Mass Spectrometry, Energy Fuels, 26, 4532–4539, https://doi.org/10.1021/ef300501t, 2012.
- McDonald, B. C., de Gouw, J. A., Gilman, J. B., Jathar, S. H., Akherati, A., Cappa, C. D., Jimenez, J. L., Lee-Taylor, J., Hayes, P. L., McKeen, S. A., Cui, Y. Y., Kim, S.-W., Gentner, D. R., Isaacman-VanWertz, G., Goldstein, A. H., Harley, R. A., Frost, G. J., Roberts, J. M., Ryerson, T. B., and Trainer, M.: Volatile chemical products emerging as largest petrochemical source of urban organic emissions, Science, 359, 760–764, https://doi.org/10.1126/science.aaq0524, 2018.
- Müller, M., Anderson, B. E., Beyersdorf, A. J., Crawford, J. H., Diskin, G. S., Eichler, P., Fried, A., Keutsch, F. N., Mikoviny, T., Thornhill, K. L., Walega, J. G., Weinheimer, A. J., Yang, M., Yokelson, R. J., and Wisthaler, A.: In situ measurements and modeling of reactive trace gases in a small biomass burning plume, Atmos. Chem. Phys., 16, 3813–3824, https://doi.org/10.5194/acp-16-3813-2016, 2016.
- O'Dell, K., Hornbrook, R. S., Permar, W., Levin, E. J. T., Garofalo, L. A., Apel, E. C., Blake, N. J., Jarnot, A., Pothier, M. A., Farmer, D. K., Hu, L., Campos, T., Ford, B., Pierce, J. R., and Fischer, E. V.: Hazardous Air Pollutants in Fresh and Aged Western US Wildfire Smoke and Implications for Long-Term Exposure, Environ. Sci. Technol., 54, 11838–11847, https://doi.org/10.1021/acs.est.0c04497, 2020.
- Pagonis, D., Sekimoto, K., and de Gouw, J.: A Library of Proton-Transfer Reactions of  $\rm H_3O^+$  Ions Used for Trace Gas Detection, J. Am. Soc. Mass Spectrom., 30, 1330–1335, https://doi.org/10.1007/s13361-019-02209-3, 2019.
- Permar, W., Wang, Q., Selimovic, V., Wielgasz, C., Yokelson, R. J., Hornbrook, R. S., Hills, A. J., Apel, E. C., Ku, I.-T., Zhou, Y., Sive, B. C., Sullivan, A. P., Collett Jr, J. L., Campos, T. L., Palm, B. B., Peng, Q., Thornton, J. A., Garofalo, L. A., Farmer, D. K., Kreidenweis, S. M., Levin, E. J. T., DeMott, P. J., Flocke, F., Fischer, E. V., and Hu, L.: Emissions of Trace Organic Gases From Western U.S. Wildfires Based on WE-CAN Aircraft Measurements, Journal of Geophysical Research: Atmospheres, 126, e2020JD033838, https://doi.org/10.1029/2020JD033838, 2021.

- Permar, W., Jin, L., Peng, Q., O'Dell, K., Lill, E., Selimovic, V., Yokelson, R. J., Hornbrook, R. S., Hills, A. J., Apel, E. C., Ku, I.-T., Zhou, Y., Sive, B. C., Sullivan, A. P., Collett, J. L., Palm, B. B., Thornton, J. A., Flocke, F., Fischer, E. V., and Hu, L.: Atmospheric OH reactivity in the western United States determined from comprehensive gas-phase measurements during WE-CAN, Environ. Sci.: Atmos., 3, 97–114, https://doi.org/10.1039/D2EA00063F, 2023.
- Pittman, C. U. Jr., Mohan, D., Eseyin, A., Li, Q., Ingram, L., Hassan, E.-B. M., Mitchell, B., Guo, H., and Steele, P. H.: Characterization of Bio-oils Produced from Fast Pyrolysis of Corn Stalks in an Auger Reactor, Energy Fuels, 26, 3816–3825, https://doi.org/10.1021/ef3003922, 2012.
- Rickly, P. S., Coggon, M. M., Aikin, K. C., Alvarez, R. J. I., Baidar, S., Gilman, J. B., Gkatzelis, G. I., Harkins, C., He, J., Lamplugh, A., Langford, A. O., McDonald, B. C., Peischl, J., Robinson, M. A., Rollins, A. W., Schwantes, R. H., Senff, C. J., Warneke, C., and Brown, S. S.: Influence of Wildfire on Urban Ozone: An Observationally Constrained Box Modeling Study at a Site in the Colorado Front Range, Environ. Sci. Technol., 57, 1257–1267, https://doi.org/10.1021/acs.est.2c06157, 2023.
- Robinson, M. A., Decker, Z. C. J., Barsanti, K. C., Coggon, M. M., Flocke, F. M., Franchin, A., Fredrickson, C. D., Gilman, J. B., Gkatzelis, G. I., Holmes, C. D., Lamplugh, A., Lavi, A., Middlebrook, A. M., Montzka, D. M., Palm, B. B., Peischl, J., Pierce, B., Schwantes, R. H., Sekimoto, K., Selimovic, V., Tyndall, G. S., Thornton, J. A., Van Rooy, P., Warneke, C., Weinheimer, A. J., and Brown, S. S.: Variability and Time of Day Dependence of Ozone Photochemistry in Western Wildfire Plumes, Environmental Science & Technology, 55, 10280–10290, https://doi.org/10.1021/acs.est.1c01963, 2021.
- Romanias, M. N., Coggon, M. M., Al Ali, F., Burkholder, J. B., Dagaut, P., Decker, Z., Warneke, C., Stockwell, C. E., Roberts, J. M., Tomas, A., Houzel, N., Coeur, C., and Brown, S. S.: Emissions and Atmospheric Chemistry of Furanoids from Biomass Burning: Insights from Laboratory to Atmospheric Observations, ACS Earth Space Chem., 8, 857–899, https://doi.org/10.1021/acsearthspacechem.3c00226, 2024.
- Román-Leshkov, Y., Barrett, C. J., Liu, Z. Y., and Dumesic, J. A.: Production of dimethylfuran for liquid fuels from biomass-derived carbohydrates, Nature, 447, 982–985, https://doi.org/10.1038/nature05923, 2007.
- Sekimoto, K., Li, S.-M., Yuan, B., Koss, A., Coggon, M., Warneke, C., and de Gouw, J.: Calculation of the sensitivity of proton-transfer-reaction mass spectrometry (PTR-MS) for organic trace gases using molecular properties, International Journal of Mass Spectrometry, 421, 71–94, https://doi.org/10.1016/j.ijms.2017.04.006, 2017.
- Selimovic, V., Ketcherside, D., Chaliyakunnel, S., Wielgasz, C., Permar, W., Angot, H., Millet, D. B., Fried, A., Helmig, D., and Hu, L.: Atmospheric biogenic volatile organic compounds in the Alaskan Arctic tundra: constraints from measurements at Toolik Field Station, Atmos. Chem. Phys., 22, 14037–14058, https://doi.org/10.5194/acp-22-14037-2022, 2022.
- Simmleit, N. and Schulten, H.-R.: Thermal degradation products of spruce needles, Chemosphere, 18, 1855–1869, https://doi.org/10.1016/0045-6535(89)90469-4, 1989.
- Stockwell, C. E., Veres, P. R., Williams, J., and Yokelson, R. J.: Characterization of biomass burning emissions from cooking

- fires, peat, crop residue, and other fuels with high-resolution proton-transfer-reaction time-of-flight mass spectrometry, Atmos. Chem. Phys., 15, 845–865, https://doi.org/10.5194/acp-15-845-2015, 2015.
- Stönner, C., Derstroff, B., Klüpfel, T., Crowley, J. N., and Williams, J.: Glyoxal measurement with a proton transfer reaction time of flight mass spectrometer (PTR-TOF-MS): characterization and calibration, Journal of Mass Spectrometry, 52, 30, https://doi.org/10.1002/jms.3893, 2016.
- Tuan Hoang, A. and Viet Pham, V.: 2-Methylfuran (MF) as a potential biofuel: A thorough review on the production pathway from biomass, combustion progress, and application in engines, Renewable and Sustainable Energy Reviews, 148, 111265, https://doi.org/10.1016/j.rser.2021.111265, 2021.
- Veres, P., Roberts, J. M., Burling, I. R., Warneke, C., de Gouw, J., and Yokelson, R. J.: Measurements of gasphase inorganic and organic acids from biomass fires by negative-ion proton-transfer chemical-ionization mass spectrometry, Journal of Geophysical Research: Atmospheres, 115, https://doi.org/10.1029/2010JD014033, 2010.
- Wang, S., Yuan, B., Wu, C., Wang, C., Li, T., He, X., Huangfu, Y., Qi, J., Li, X.-B., Sha, Q., Zhu, M., Lou, S., Wang, H., Karl, T., Graus, M., Yuan, Z., and Shao, M.: Oxygenated volatile organic compounds (VOCs) as significant but varied contributors to VOC emissions from vehicles, Atmos. Chem. Phys., 22, 9703–9720, https://doi.org/10.5194/acp-22-9703-2022, 2022.
- Warneke, C., Veres, P., Holloway, J. S., Stutz, J., Tsai, C., Alvarez, S., Rappenglueck, B., Fehsenfeld, F. C., Graus, M., Gilman, J. B., and de Gouw, J. A.: Airborne formaldehyde measurements using PTR-MS: calibration, humidity dependence, intercomparison and initial results, Atmos. Meas. Tech., 4, 2345–2358, https://doi.org/10.5194/amt-4-2345-2011, 2011a.
- Warneke, C., Roberts, J. M., Veres, P., Gilman, J., Kuster, W. C., Burling, I., Yokelson, R., and de Gouw, J. A.: VOC identification and inter-comparison from laboratory biomass burning using PTR-MS and PIT-MS, International Journal of Mass Spectrometry, 303, 6–14, https://doi.org/10.1016/j.ijms.2010.12.002, 2011b.
- Yokelson, R. J., Burling, I. R., Gilman, J. B., Warneke, C., Stockwell, C. E., de Gouw, J., Akagi, S. K., Urbanski, S. P., Veres, P., Roberts, J. M., Kuster, W. C., Reardon, J., Griffith, D. W. T., Johnson, T. J., Hosseini, S., Miller, J. W., Cocker III, D. R., Jung, H., and Weise, D. R.: Coupling field and laboratory measurements to estimate the emission factors of identified and unidentified trace gases for prescribed fires, Atmos. Chem. Phys., 13, 89–116, https://doi.org/10.5194/acp-13-89-2013, 2013.
- Yuan, B., Koss, A., Warneke, C., Gilman, J. B., Lerner, B. M., Stark, H., and de Gouw, J. A.: A high-resolution time-of-flight chemical ionization mass spectrometer utilizing hydronium ions (H<sub>3</sub>O<sup>+</sup> ToF-CIMS) for measurements of volatile organic compounds in the atmosphere, Atmos. Meas. Tech., 9, 2735–2752, https://doi.org/10.5194/amt-9-2735-2016, 2016.
- Yuan, B., Koss, A. R., Warneke, C., Coggon, M., Sekimoto, K., and de Gouw, J. A.: Proton-Transfer-Reaction Mass Spectrometry: Applications in Atmospheric Sciences, Chem. Rev., 117, 13187– 13229, https://doi.org/10.1021/acs.chemrev.7b00325, 2017.